A 10^9 neutrons/pulse transportable pulsed D-D neutron source based on flexible head plasma focus unit

Ram Niranjan, R. K. Rout, R. Srivastava, T. C. Kaushik, and Satish C. Gupta

Citation: Rev. Sci. Instrum. **87**, 033504 (2016); doi: 10.1063/1.4942666
View online: http://dx.doi.org/10.1063/1.4942666
View Table of Contents: http://aip.scitation.org/toc/rsi/87/3
Published by the American Institute of Physics

A 10^9 neutrons/pulse transportable pulsed D-D neutron source based on flexible head plasma focus unit

Ram Niranjan,[a] R. K. Rout, R. Srivastava, T. C. Kaushik, and Satish C. Gupta
Applied Physics Division, Bhabha Atomic Research Centre, Mumbai 400 085, India

(Received 3 August 2015; accepted 11 February 2016; published online 10 March 2016)

A 17 kJ transportable plasma focus (PF) device with flexible transmission lines is developed and is characterized. Six custom made capacitors are used for the capacitor bank (CB). The common high voltage plate of the CB is fixed to a centrally triggered spark gap switch. The output of the switch is coupled to the PF head through forty-eight 5 m long RG213 cables. The CB has a quarter time-period of 4 μs and an estimated current of 506 kA is delivered to the PF device at 17 kJ (60 μF, 24 kV) energy. The average neutron yield measured using silver activation detector in the radial direction is $(7.1 \pm 1.4) \times 10^8$ neutrons/shot over 4π sr at 5 mbar optimum D_2 pressure. The average neutron yield is more in the axial direction with an anisotropy factor of 1.33 ± 0.18. The average neutron energies estimated in the axial as well as in the radial directions are (2.90 ± 0.20) MeV and (2.58 ± 0.20) MeV, respectively. The flexibility of the PF head makes it useful for many applications where the source orientation and the location are important factors. The influence of electromagnetic interferences from the CB as well as from the spark gap on applications area can be avoided by putting a suitable barrier between the bank and the PF head. © *2016 AIP Publishing LLC.* [http://dx.doi.org/10.1063/1.4942666]

I. INTRODUCTION

Plasma focus (PF) devices have long been studied in different laboratories across the world since their inception independently by Fillipov[1] and by Mather.[2] They operate by producing fast electrical discharge between a pair of coaxial electrodes fixed inside a chamber. The device acts as a coaxial plasma accelerator gun in which the Lorentz force drives the plasma sheath in the annular space between the electrodes, making it collapse at the open end of the symmetry axis forming hot and dense plasma. This results in emission of an intense pulse of electromagnetic radiation as well as stream of energetic ions and relativistic electrons. The neutrons are produced through fusion reactions if deuterium (D_2) or deuterium-tritium (DT) mixture is used as the working gas.

Having been studied for more than five decades, both theoretically and experimentally, the PF device is still a fascinating field of research, due to the richness of underlying physics as well as its potential applications, e.g., explosives and contraband detection,[3] radio-isotopes production,[4] and flash X-ray radiography.[5] Realizing the potentials of the PF device, it has been designed and operated in various energy ranges varying from less than a joule to mega-joules.[6–28] In the PF devices, the energy stored in the capacitor bank (CB) is transferred to the PF head through a spark gap (SG) switch either using parallel flat plate transmission lines or using a number of coaxial cables connected in parallel. While the first scheme makes the complete system compact in geometry, easy in maintenance and more economical, the latter has advantage in terms of higher flexibility of keeping and moving the PF head at any location and orientation conveniently as per the required application. In the mega-joule device (PF-1000) at the IPPLM (Institute of Plasma Physics and Laser Micro fusion), Poland,[20] the electrical energy stored in the 1.332 mF CB (1064 kJ, 40 kV) is transferred to the collector plate of the PF head using low inductance cables. Though it is cable based, it is stationary due to the large CB and the PF head. Mathuthu *et al.*[21] have developed a 2.3 kJ (32.6 μF, 12 kV) device where the PF head is connected to the CB of single capacitor using sixteen 1 m long coaxial cables. Freeman *et al.*[22] have developed TAMU 460 kJ (44.4 μF, 60 kV) PF device. The CB for the 460 kJ PF device is divided into six modules. The energy of each module is discharged to the PF head through seventy-two RG17/14 coaxial cables. Borthakur *et al.*[23] have used two-electrode parallel plate SG switch to operate a 5 kJ PF device. One side of the SG switch is screwed to the central electrode (anode) of the PF head and the other side is connected to the CB with thirty-two RG213 coaxial cables. All the above mentioned devices are stationary either due to short cables or bulkiness of the CB and the PF head, which restrict the movement and orientation of the neutron source. Several PF devices[29–33] have been developed by us and are operated for different applications. A compact 11.5 kJ PF device[33] was developed in which the CB (40 μF, 24 kV) is discharged to the PF head through a SG switch using flat plate transmission lines. In this device, the central electrode was working as one end of the SG switch. It was used for non-destructive assay of nuclear fissile materials (U^{235}) by the delayed gamma[34] and the delayed neutron counting.[35] Here we report the development of a 17 kJ PF device in which PF head is connected to the CB using forty-eight 5 m long flexible RG213 coaxial cables and to the vacuum system through a 5 m long flexible stainless-steel (SS) bellow. The flexibility of the cables and not so heavy weight of the PF head permit the positioning of neutron source at any convenient orientation for special applications.[34,35] The

[a]Email: niranjan@barc.gov.in

flexibility of the PF head is incorporated for the first time in such type of unit. Moreover, the interference in various measurements due to high electromagnetic noise generated during the triggering of the spark gap and discharge of the CB can also be avoided by putting an appropriate barrier. The details of the design of the 17 kJ PF device along with the neutron emission characteristics are reported.

II. DESCRIPTIONS OF SETUP

A. The capacitor bank

The capacitor bank consists of six custom made capacitors (10 μF, 25 nH, 25 kV each) capable of delivering 506 kA current at 17 kJ (60 μF, 24 kV) energy of operation. The capacitors are connected in parallel through a common collector plate made of SS. One end of an open air SG switch is directly connected to this plate and other end is fixed to another parallel flat plate. This flat plate is connected to the PF head through forty-eight RG213 coaxial cables of 5 m length each. The numbers of coaxial cables are optimized for the minimization of system inductance and convenience in mechanical assembly. The weight of all the coaxial cables is around 40 kg. The weight of the CB (including SG assembly) is around 325 kg and it is placed over a movable trolley. The weight of the PF head along with the experimental chamber is around 35 kg. Thus the weight of the complete system with CB, spark gap assembly, PF unit, and coaxial cables is around 400 kg. The CB is charged to the required voltage using a compact high voltage power supply. The power supply is remotely operated through a hand held control panel. A negative pulse of 30 kV with <1 μs rise time is used to trigger the SG switch.

B. The plasma focus device

The schematic of the complete system is shown in Figure 1(a). It is drawn with arbitrary scale to bring out clarity of important features. The electrode assembly of the PF unit

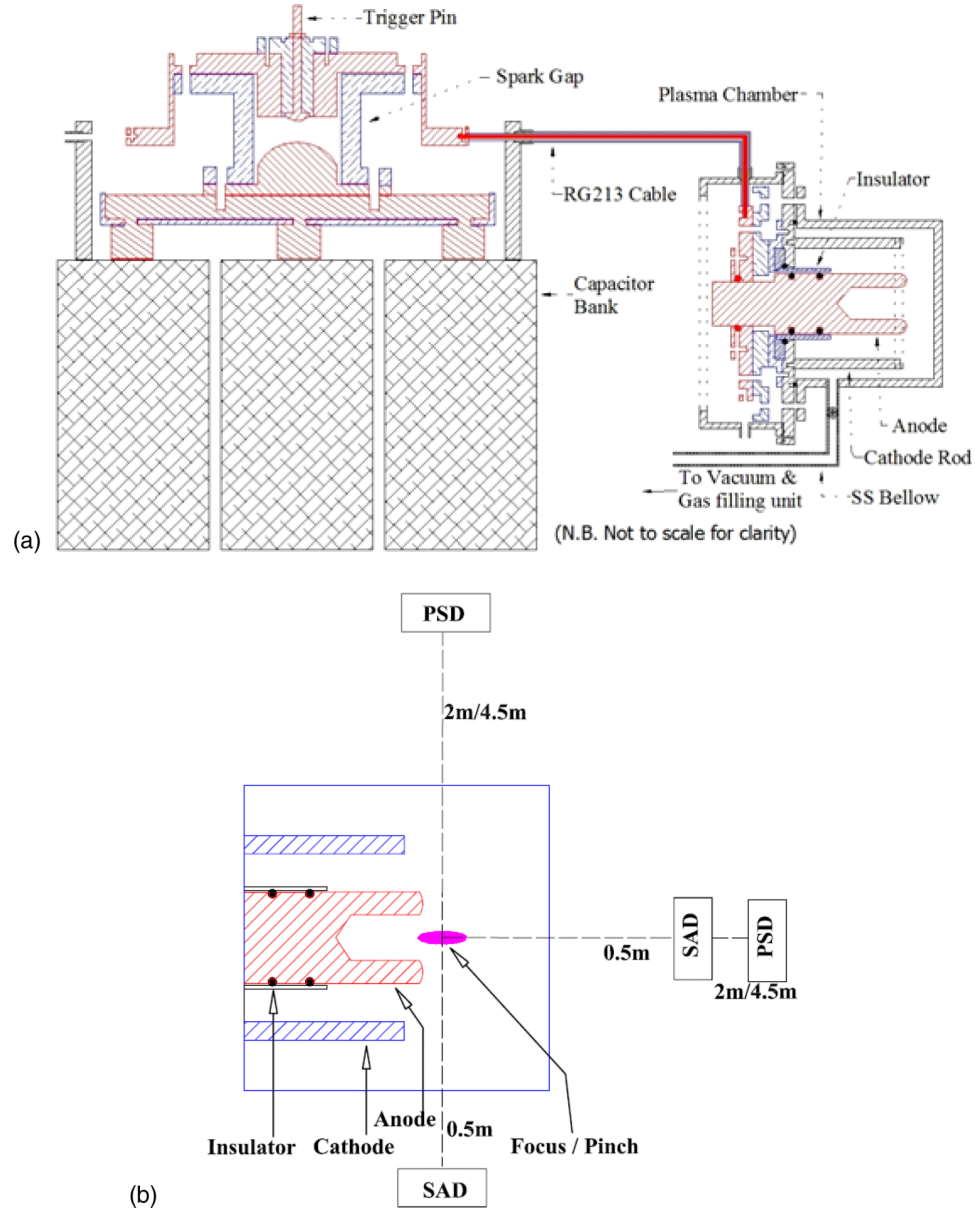

FIG. 1. (a) A schematic of the plasma focus device setup. (b) A layout of the employed diagnostic setup.

is of squirrel cage geometry. Dimensions of the electrodes have been chosen so that the axial run down time of the plasma sheath matches with the quarter time-period of the CB discharge current as described in the snowplow model for the axial phase. The characteristic axial transit time of the plasma sheath is taken as[36]

$$t_a = \left(\frac{4\pi^2 (b^2 - a^2) z_0^2 \rho}{\mu \ln (b/a) I_0^2} \right)^{1/2}. \quad (1)$$

Here I_0 is peak current, ρ is mass density of the gas, μ is permeability of the free space, and a and b are radius of the inner electrode (anode) and the outer electrode (cathode), respectively. The quarter time-period of the discharge current can be estimated using $[\pi(L_0C_0)^{1/2}]/2$, where L_0 and C_0 are the static inductance and the capacitance of the system. The electrodes are made of SS and their dimensions are chosen for operations at 24 kV voltage. The exposed length and the diameter of the anode are 77 mm and 60 mm, respectively. The cathode consists of twelve rods (12 mm diameter each) fixed around the anode. The annular spacing between the anode and the cathode is 25 mm for efficient snowplowing of the plasma and the neutral gas by the accelerating plasma sheath in the run down phase. The anode has been given hollow shape at the tip to avoid erosion due to relativistic electrons accelerated in downward direction in the post pinch phase. The effective length of the quartz insulator is chosen around 4 kV/cm of the operating voltage, viz., 54 mm for uniform plasma sheath formation in the initial breakdown phase.[37–39]

C. The experimental plasma chamber

The PF electrode assembly is mounted inside a high vacuum compatible experimental plasma chamber. One of the side ports of the chamber is used for evacuation and gas filling during the PF device operation. The experimental chamber is connected to a diffstac (diffusion pump with rotary pump) high vacuum pumping system through a flexible SS bellow of 5 m length. The chamber is also connected to the D_2 gas storage cylinder having a Swagelok make bellow sealed valve through a 6 mm diameter flexible copper tube for D_2 gas filling. During experiments, this chamber is evacuated to a base pressure of $\leq 10^{-5}$ mbar and then filled with D_2 gas to the desired pressure of a few mbar. The filling gas pressure was measured using an Edward make capsule dial gauge (0-25 mbar pressure range).

D. Diagnostics

The current derivative (dI/dt) waveform was monitored using a Rogowsky coil. The dI/dt waveform was integrated to get current [I(t)] waveform with a calibration factor of 1500 kA/V. The voltage signal was measured using resistive divider made of copper sulphate ($CuSO_4$) solution. Two silver activation detectors (SADs) were kept at a distance of 0.5 m from the PF anode tip in the axial [along (0°) to the anode axis] direction and the radial [perpendicular (90°) to the anode axis] for the neutron yield (Y_n) measurement. The neutron yield anisotropy $[Y_n(0°)/Y_n(90°)]$ was estimated. Both the SADs were *in situ* calibrated using a Pu-Be neutron source of known strength. Two identical plastic scintillator detectors (PSDs) were kept in the axial and in the radial directions for time resolved hard X-rays and neutron measurements. Time of flight (TOF) method was used to estimate neutron energy. Each PSD was having a NE102A plastic scintillator of 50 mm diameter and 50 mm thickness coupled to an XP2012 (Philips) photomultiplier tube. Both the detectors were placed in the same direction and at the same distance from PF head for a few PF shots for synchronization study. All the time resolved signals were recorded in a digital storage oscilloscope having 1 GHz bandwidth and 5 GS/s sampling rate. This was placed inside a Faraday cage. The layout of the employed diagnostic set up is shown in Figure 1(b).

III. RESULTS AND DISCUSSION

A. Short circuit inductance measurement

The plasma focus electrodes were shorted at the top to measure the short circuit time period and inductance of the complete system. The inductance ($L_0 = T^2/4\pi^2C_0$) and the peak current $[I_0 = V_0(kC_0/L_0)^{0.5}]$ at V_0 voltage were estimated from the time period (T) and the voltage reversal (k) values measured using short circuit current derivative signal. All forty-eight RG213 cables were added in multiple steps. At each step, the time period was measured. As expected, the inductance reduced with the increasing number of cables as shown in Figure 2. The inductance decreased by a factor of 2.6 from 1080 nH for two cables to 421 nH for six cables. It further decreased by a factor of 2.5, i.e., to 169 nH for twenty-four cables. The variation of inductance (L) with number of cables could be fitted using a power function as

$$L = A + B \cdot N^C, \quad (2)$$

where N is the number of RG213 cable. A, B, and C are constants given in Table I.

This closely matches with the expected variation of inductance of a system having fixed inductance A and N number of cables each of inductance B. Forty-eight cables have been chosen for the minimum possible inductance of the PF system and for convenience in mechanical assembly. The short circuit time period and the inductance with forty-eight cables are 16 μs and

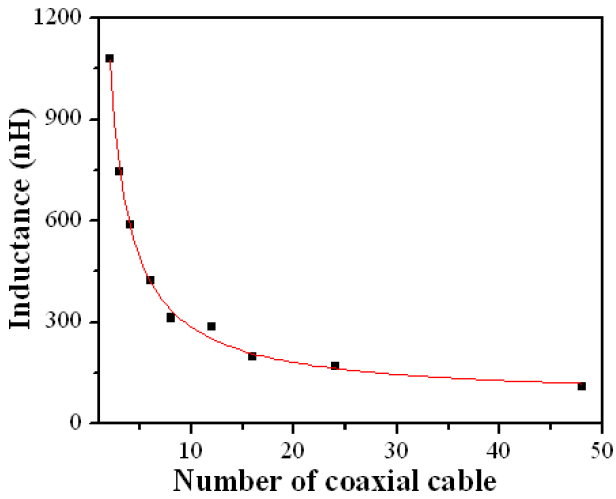

FIG. 2. Variation in short circuit inductance of plasma focus device with numbers of coaxial cables.

TABLE I. Values of fitting parameter and standard error.

Constant	Value	Standard error
A	71.41	21.3
B	1962.03	74.3
C	−0.96	−0.06

108 nH, respectively. Maximum current of 506 kA is estimated to be discharged to the PF unit at 24 kV charging voltage.

B. Neutrons and hard X-ray measurement

The PF device was operated with D_2 gas at pressure range of 3–8 mbar at 17 kJ CB energy. Typical signals of current derivative (dI/dt), current [I(t)], and voltage [V(t)] are shown in Figure 3. This device has been operated for more than 500 shots with an average of eight to ten shots per day. Each shot was taken with fresh D_2 gas filling at the desired pressure. A time gap of around 15 min was maintained between two shots. This time gap is necessary to provide sufficient time for cooling of the quartz insulator after the shot as this heats up[40] in the initial breakdown phase. The observed maximum neutron yield was 8.4×10^8 neutrons/shot over 4π sr at 5 mbar D_2 pressure using SAD detector kept in the radial direction The reported neutron yields as per the various scaling laws for

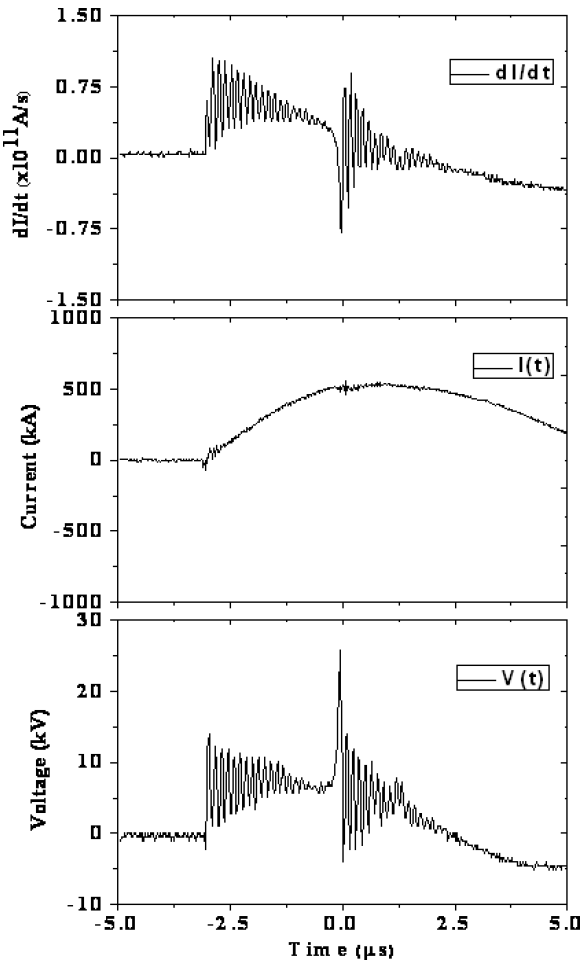

FIG. 3. Typical current derivative (dI/dt), current [I(t)], and voltage [V(t)] signals.

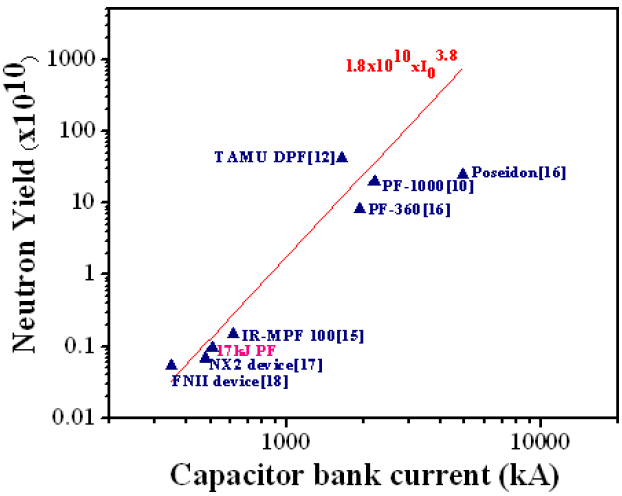

FIG. 4. Average neutron yields of various plasma focus devices (ref. in bracket). The straight red line shows the scaling law.

PF devices are $Y_n \approx 1.7 \times 10^{-10} \times I_0^{3.3}$ (with I_0 is in Amp)[41] or $Y_n \approx 1.8 \times 10^{10} \times I_0^{3.8}$ (I_0 is 0.3–5.7 MA).[42] The neutron yields estimated from the given scaling laws at 506 kA current are 1.13×10^9 neutrons/shot and 1.35×10^9 neutrons/shot, respectively. It is close to experimentally measured neutron yield in our 17 kJ PF device. The neutron yields from the PF devices in other laboratories along with our 17 kJ PF device are plotted in Figure 4 for comparison.

The average neutron yield was evaluated at all D_2 pressures. Variation in the neutron yield in the radial direction with the D_2 pressures at 17 kJ energy is shown in Figure 5. The average neutron yield increases to maximum of $(7.1 \pm 1.4) \times 10^8$ neutrons/shot at 5 mbar pressure (optimum pressure) and it starts decreasing with further increase in D_2 pressure. The average values are estimated from 10 consecutive PF shots at each D_2 pressure. The neutron yield anisotropy Y_0°/Y_{90}° (ratio of the neutron yield in the axial direction to the radial direction) has also been evaluated. The neutron yield anisotropy increases with increase in D_2 gas pressure reaching a maximum at 5 mbar and then decreases with further increase in pressure as shown in Figure 6. The maximum neutron yield anisotropy

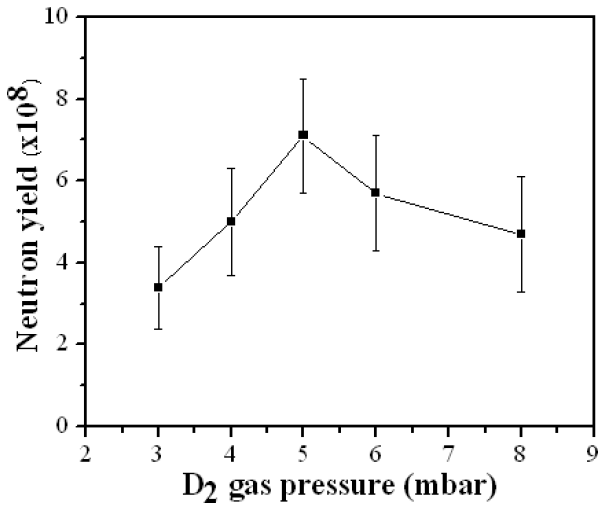

FIG. 5. Variation in neutron yield in radial direction with deuterium gas pressure.

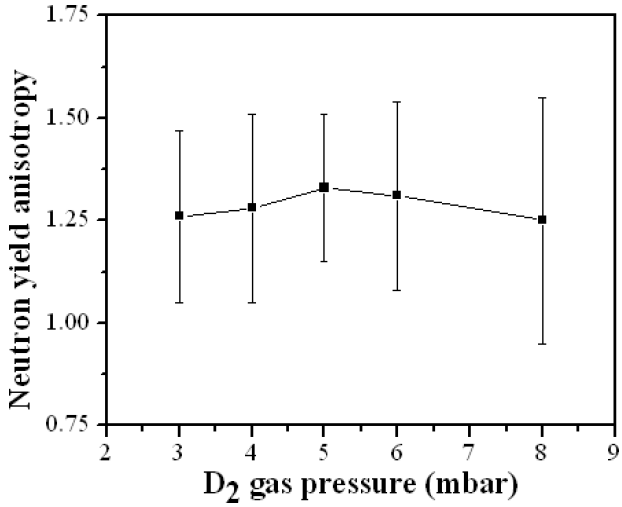

FIG. 6. Variation in neutron yield anisotropy with deuterium gas pressure.

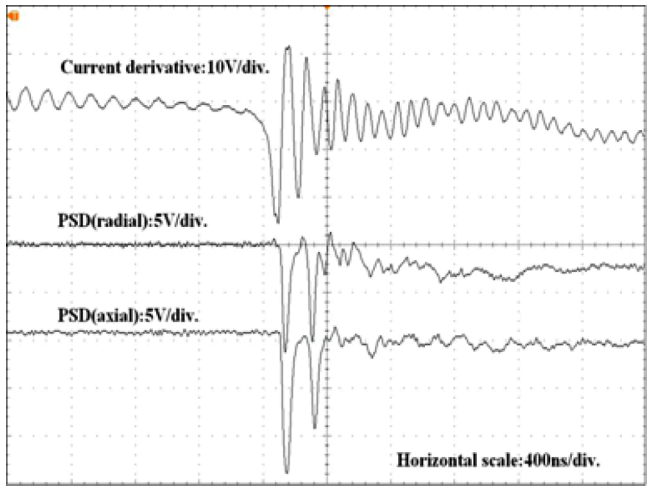

FIG. 8. Typical current derivative, time resolved hard X-rays, and neutron signals at 4.5 m distance in the radial as well as in the axial directions.

is of 1.33 ± 0.18 at 5 mbar D_2 gas pressure. The possible reason for neutron yield anisotropy is beam-target mechanism for neutron production. The variation in neutron yield anisotropy with D_2 pressure is due to variation in energy spectrum of deuterium ions responsible for the beam-target fusion.[24]

Typical signals from the pickup loop as well as through the PSDs at 2 m distance in the axial and radial directions are displayed in Figure 7. Similar signals at 4.5 m distance are shown in Figure 8. The first peak is due to the hard X-rays and the second peak is due to the neutrons. It was observed that the X-rays were completely or maximum attenuated by putting a 50 mm thick lead block in front of the PSDs. The neutron peak was also reaffirmed by the TOF separation between two peaks (X-rays and neutrons) which changed by changing the distance of the PSD from the PF device. The TOF was used to estimate neutron energy in both the directions (assuming that the neutrons and hard X-rays were generated at the same time). The energy of neutrons produced from D-D nuclear fusion reactions through thermonuclear mechanism is expected to be close to 2.45 MeV. The evaluated TOF separations for 2.45 MeV neutron at 2 m and 4.5 m are supposed to be 86 ns and 193 ns, respectively. But the observed different separation time implies that the neutron energy is more than 2.45 MeV in both the directions. Moreover, the neutron energy estimated from the TOF separation is more in the axial direction compared to the radial direction. Higher neutron energies (greater than 2.45 MeV) suggest non-thermal process (beam-target mechanism) of neutron production in the PF device. The neutron energy varies in both the directions with the change in D_2 gas pressure. The neutron energy anisotropy E_0°/E_{90}° (i.e., ratio of the neutron energies in the axial to radial directions) was estimated using signals from two PSDs in the axial and in the radial directions, respectively, at different D_2 gas pressures. The variation of neutron energy anisotropy as a function of D_2 gas pressure is shown in Figure 9. The neutron energy anisotropy initially increases with increase in D_2 gas pressure reaching a maximum of 1.35 ± 0.09 at 5 mbar and then decreases with further increase in pressure. The average values of neutron energies in the axial and the radial directions are also found to be maximum at 5 mbar D_2 pressure and the corresponding values are (2.90 ± 0.20) MeV and (2.58 ± 0.20) MeV, respectively. The variations in the

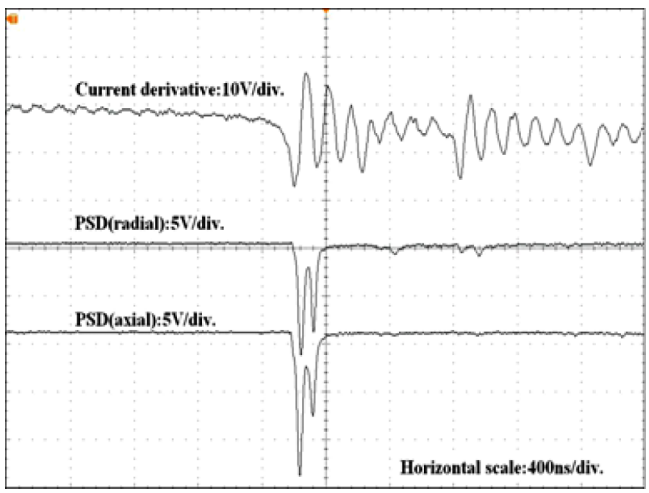

FIG. 7. Typical current derivative, time resolved hard X-rays, and neutron signals at 2 m distance in the radial and the axial directions.

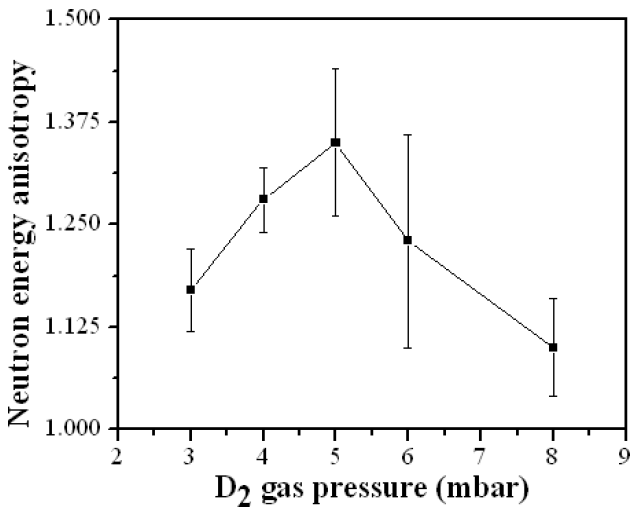

FIG. 9. Variation in neutron energy anisotropy with deuterium gas pressure.

neutron energy anisotropy show similar trends with the filling pressure as that of the neutron yield anisotropy. The possible reason may be that the accelerated deuterium ions, which are responsible for the beam-target neutron emission,[24,43,44] have higher energy and fluence in the axial direction compared to the radial direction at different filling gas pressures.

The pulse durations, i.e., full width at half maximum (FWHM) as well as intensities of the hard X-rays and neutrons were measured in both the directions as a function of D_2 gas filling pressure and at a distance of 2 m from the tip of the PF anode. It was found to be more in the axial direction compared to the radial direction. The average pulse durations of the hard X-rays in the axial and the radial directions are (47 ± 6) ns and (42 ± 3) ns, respectively, at optimum 5 mbar D_2 pressure. The average pulse durations of neutrons in respective directions are (42 ± 6) ns and (39 ± 5) ns, respectively, at optimum pressure.

IV. CONCLUSION

A transportable pulsed neutron source based on a flexible plasma focus head has been developed. The PF head is connected to the CB using forty-eight 5 m long RG213 cables and to the vacuum pumping system using 5 m long SS bellow. The total inductance of the unit is 108 nH and the maximum current estimated to be delivered to the PF head is 506 kA. The PF device was operated from 3 to 8 mbar of D_2 gas pressure. The average neutron yield is (7.1 ± 1.4) $\times 10^8$ neutrons/shot over 4π sr with average neutron yield anisotropy of 1.33 ± 0.18 at 5 mbar D_2 pressure (optimum pressure). The average neutron energies in the axial and radial directions are (2.90 ± 0.20) MeV and (2.58 ± 0.20) MeV, respectively, at same D_2 pressure (5 mbar). The coincidence of the maximum neutron yield and the maximum neutron energy indicates beam-target interaction of accelerated deuterium ions with the background neutral gas in the experimental chamber. The variation in neutron yield anisotropy and neutron energy anisotropy with D_2 pressure is possibly due to variation in energy spectrum of deuterium ions responsible for beam-target fusion.

The separation of PF head from the CB makes the PF device safe in operation. It also reduces the interference caused in the signals due to high electromagnetic noises generated during the CB discharge. Moreover, the mechanical vibrations of the triggered spark gap do not get transferred to the insulator due to the separation of the CB and PF head. This will enhance the life of ceramic insulators. This PF device has been operated for more than 500 shots without changing the quartz insulator. This PF device may prove to be useful for applications where the location and the orientation of the neutron source are important factors.

ACKNOWLEDGMENTS

The authors would like to thank Ms. Varsha Kale and Mr. Kanchan Bonde for their technical assistance in operation of the plasma focus device.

[1]N. V. Filippov, T. I. Filippova, and V. P. Vinogradov, "Dense, high-temperature plasma in a non-cylindrical z-pinch compression," Nucl. Fusion, Suppl. 2, 577–587 (1962).
[2]J. W. Mather, "Formation of a high-density deuterium plasma focus," Phys. Fluids **8**(2), 366–377 (1965).
[3]V. A. Gribkov, S. V. Latyshev, R. A. Miklaszewski, M. Chernyshova, K. Drozdowicz, U. Wiacek, K. Tomaszewski, and B. D. Lemeshko, "A dense plasma focus-based neutron source for a single-shot detection of illicit materials and explosives by a nanosecond neutron pulse," Phys. Scr. **81**, 035502 (2010).
[4]M. V. Roshan, S. V. Springham, R. S. Rawat, and P. Lee, "Short-lived PET radioisotope production in a small plasma focus device," IEEE Trans. Plasma Sci. **38**(12), 3393–3397 (2010).
[5]F. D. Lorenzo, V. Raspa, P. Knoblauch, A. Lazarte, C. Moreno, and A. Clausse, "Hard x-rays source for flash radiography based on a 2.5 kJ plasma focus," J. Appl. Phys. **102**, 033304 (2007).
[6]L. Soto, C. Pavez, A. Tarifeno, J. Moreno, and F. Veloso, "Studies on scalability and scaling laws for the plasma focus: Similarities and differences in devices from 1 MJ to 0.1 J," Plasma Sources Sci. Technol. **19**(5), 055017 (2010).
[7]L. Soto, "New trends and future perspectives on plasma focus research," Plasma Phys. Controlled Fusion **47**(5A), A361 (2005).
[8]L. Soto, C. Pavez, J. Moreno, M. Barbaglia, and A. Clausse, "Nanofocus: Ultra-miniature dense pinch plasma focus device with submillimetric anode operating at 0.1 J," Plasma Sources Sci. Technol. **18**, 015007 (2009).
[9]C. Pavez and L. Soto, "Demonstration of x-ray emission from an ultraminiature pinch plasma focus discharge operating at 0.1 J. Nanofocus," IEEE Trans. Plasma Sci. **38**, 1132 (2010).
[10]L. Soto, C. Pavez, J. Moreno, A. Tarifeno, J. Pedreros, and L. Altamirano, "Nanofocus of tenth of joules and portable plasma focus of few joules for field applications," AIP Conf. Proc. **1088**, 219 (2009).
[11]L. Soto, C. Pavez, J. Moreno, J. Pedreros, and L. Altamirano, "Non-radioactive source for field applications based in a plasma focus of 2 J: Pinch evidence," J. Phys.: Conf. Ser. **511**, 12032 (2014).
[12]P. Silva, L. Soto, W. Kies, and J. Moreno, "Pinch evidence in a fast and small plasma focus of only tens of joules," Plasma Sources Sci. Technol. **13**, 329 (2004).
[13]L. Soto, P. Silva, J. Moreno, M. Zambra, W. Kies, R. E. Mayer, A. Clausse, A. Altamirano, C. Pavez, and L. Huerta, "Demonstration of neutron production in a table top pinch plasma focus device operated at only tens of joules," J. Phys. D: Appl. Phys. **41**, 205215 (2008).
[14]M. O. Barbaglia, H. Bruzzone, H. A. Nestor, L. Soto, and A. Clausse, "Electrical behavior of an ultralow-energy plasma focus," IEEE Trans. Plasma Sci. **42**, 138 (2014).
[15]S. R. Mohanty, T. Sakamoto, Y. Kobayashi, I. Song, M. Watanabe, T. Kawamura, A. Okino, K. Horioka, and E. Hotta, "Miniature hybrid plasma focus extreme ultraviolet source driven by 10 kA fast current pulse," Rev. Sci. Instrum. **77**, 043506 (2006).
[16]M. Milanese, R. Moroso, and J. Pouzo, "D-D neutron yield in the 125 J dense plasma focus nanofocus," Eur. Phys. J. D **27**, 77 (2003).
[17]P. Silva, J. Moreno, L. Soto, L. Birstein, R. Mayer, and W. Kies, "Neutron emission from a fast plasma focus of 400 Joules," Appl. Phys. Lett. **83**, 3269 (2003).
[18]V. A. Gribkov, B. Bienkowska, M. Borowiecki, V. Dubrovsky, I. Ivanova-Stanik, L. Karpinski, R. A. Miklaszewski, M. Paduch, M. Scholz, and K. Tomaszewski, "Plasma dynamics in PF-1000 under full-scale energy storage. I. Pinch dynamics, shock-wave diffraction and inertial electrode," J. Phys. D: Appl. Phys. **40**, 1977 (2007).
[19]V. A. Gribkov *et al.*, "Plasma dynamics in PF-1000 under full-scale energy storage: II. Fast electron and ion characteristics versus neutron emission parameters and gun optimization perspectives," J. Phys. D: Appl. Phys. **40**, 3592 (2007).
[20]M. Scholz, R. A. Miklaszewski, V. A. Gribkov, and F. Mezzetti, "PF-1000 device," Nukleonika **45**(3), 155–158 (2000).
[21]M. Mathuthu, T. G. Zengeni, and A. V. Gholap, "Design, fabrication, and characterization of a 2.3 kJ plasma focus of negative inner electrode," Rev. Sci. Instrum. **68**(3), 1429 (1997).
[22]B. L. Freeman, J. Boydston, J. Ferguson, T. Guy, B. Lindeburg, A. Luginbill, and J. Rock, "Preliminary neutron scaling of the TAMU 460 kJ plasma focus," in Proceedings of the 27th IEEE International Conference Pulsed Power Plasma Science, New Orleans, LA, 594, 2001.
[23]T. K. Borthakur and A. Shyam, "Analysis of axial neutron emission pulse from a plasma focus device," Indian J. Pure Appl. Phys. **48**, 100–103 (2010).
[24]R. Verma, R. S. Rawat, P. Lee, M. Krishnan, S. V. Springham, and T. L. Tan, "Experimental study of neutron emission characteristics in a compact sub-kilojoule range miniature plasma focus device," Plasma Phys. Controlled Fusion **51**, 075008 (2009).

[25]A. Salehizadeh *et al.*, "Preliminary results of the 11.5 kJ dense plasma focus device IR-MPF-100," J. Fusion Energy **32**, 293 (2013).
[26]H. Herold, A. Jerzykiewicz, M. Sadowski, and H. Schmidt, "Comparative analysis of large plasma focus experiments performed at IPF, Stuttgart and at IPJ, Swierk," Nucl. Fusion **29**(8), 1255 (1989).
[27]A. Patran, R. S. Rawat, J. M. Koh, S. V. Springham, T. L. Tan, P. Lee, and S. Lee, "A high flux pulsed neutron source using a plasma focus device," in *Proceedings of the 31st EPS Conference on Plasma Physics* (Imperial College, London, 2004), p. 4.213.
[28]F. C. Mejia, I. G. Buen, J. J. E. Herrera-Velázquez, and J. Rangel-Gutiérrez, "Neutron emission characterization at the FN-II dense plasma focus device," J. Phys.: Conf. Ser. **511**, 012021 (2014).
[29]R. Niranjan, R. K. Rout, P. Mishra, R. Srivastava, A. M. Rawool, T. C. Kaushik, and S. C. Gupta, "Note: A portable pulsed neutron source based on the smallest sealed-type plasma focus device," Rev. Sci. Instrum. **82**, 026104 (2011).
[30]R. K. Rout, R. Niranjan, P. Mishra, R. Srivastava, A. M. Rawool, T. C. Kaushik, and S. C. Gupta, "Palm top plasma focus device as a portable pulsed neutron source," Rev. Sci. Instrum. **84**(6), 063503 (2013).
[31]R. K. Rout, P. Mishra, A. M. Rawool, L. V. Kulkarni, and S. C. Gupta, "Battery powered tabletop pulsed neutron source based on a sealed miniature plasma focus device," J. Phys. D: Appl. Phys. **41**, 205211 (2008).
[32]R. Niranjan, R. K. Rout, R. Srivastava, and S. C. Gupta, "The smallest plasma accelerator device as a radiation safe repetitive pulsed neutron source," Indian J. Pure Appl. Phys. **50**, 785 (2012).
[33]R. Niranjan, R. K. Rout, R. Srivastava, and S. C. Gupta, "Development and study of 13 kJ capacitor bank and plasma focus device," in *25th National Symposium Plasma Science and Technology (PLASMA-2010), Guwahati, India, Dec 8-11, 2010* (Institute of Advanced Study in Science & Technology (IASST), Guwahati, India, 2010), p. 79.
[34]S. Andola, R. Niranjan, T. C. Kaushik, R. K. Rout, A. Kumar, D. B. Paranjape, P. Kumar, B. S. Tomar, K. L. Ramakumar, and S. C. Gupta, "Use of delayed gamma rays for active non-destructive assay of ^{235}U irradiated by a pulse neutron source (plasma focus)," Nucl. Instrum. Methods Phys. Res., Sect. A **753**, 138–142 (2014).
[35]B. S. Tomar, T. C. Kaushik, S. Andola, R. Niranjan, R. K. Rout, A. Kumar, D. B. Paranjape, P. Kumar, K. L. Ramakumar, S. C. Gupta, and R. K. Sinha, "Non-destructive assay of fissile materials through active neutron interrogation technique using pulsed neutron (plasma focus) device," Nucl. Instrum. Methods Phys. Res., Sect. A **703**, 11–15 (2013).
[36]S. Lee and A. Serban, "Dimensions and lifetime of the plasma focus pinch," IEEE Trans. Plasma Sci. **24**(3), 1101–1105 (1996).
[37]M. Zakaullah, G. Murtaza, I. Ahmad, F. N. Beg, M. M. Beg, and M. Shabbir, "Comparative study of low energy plasma focus devices," Plasma Source Sci. Technol. **4**, 117–124 (1995).
[38]H. R. Yousefi, F. M. Aghamir, and K. Masugata, "Effect of the insulator length on Mather-type plasma focus devices," Phys. Lett. A **361**, 360–363 (2007).
[39]R. K. Rout, A. B. Garg, A. Shyam, and M. Srinivasan, "Influence of electrode and insulator materials on the neutron emission in a low energy plasma focus device," IEEE Trans. Plasma Sci. **23**(6), 996–1000 (1995).
[40]H. Bruzzone and R. Vieytes, "The initial phase in plasma focus devices," Plasma Phys. Controlled Fusion **35**, 1745–1754 (1993).
[41]H. Schmidt, "The plasma focus-a review," Atomkernenergie Kerntechnik **36**(3), 161–166 (1980).
[42]S. H. Saw and S. Lee, "Scaling laws for plasma focus machines from numerical experiments," Energy Power Eng. **2**(1), 65–72 (2010).
[43]M. J. Bernstein and G. G. Comisar, "Neutron energy and flux distributions from a crossed-field acceleration model of plasma focus and Z-pinch discharge," Phys. Fluids **15**(4), 700–707 (1972).
[44]M. J. Bernstein, C. M. Lee, and F. Hai, "Time correlations of x-ray spectra with neutron emission from a plasma-focus discharge," Phys. Rev. Lett. **27**(13), 844–847 (1971).